



## MODELING OF CYCLIC RESPONSE OF SHALLOW FOUNDATIONS WITH WINKLER MODEL: SOME ISSUES

N. Allotey<sup>1</sup> and M. H. El Naggar<sup>2</sup>

### ABSTRACT

Shallow foundations undergo rocking, sliding and settlement under lateral cyclic motion. The Winkler foundation model is mainly used in modeling pile foundations, but can also be used to model shallow foundations. This paper explores the strengths and limitations of the method when used in modeling the cyclic response of shallow foundations. This is accomplished by using a generalized Winkler model recently developed at the University of Western Ontario to simulate the cyclic response of a shallow foundation cyclic test conducted at the centrifuge facility of the Center for Geotechnical Modeling at the University of California at Davis.

### Introduction

Soil-structure interaction (SSI) effects are often neglected when using traditional code force-based seismic design approaches, since its effects are judged to be beneficial. This can be attributed to the fact that the consideration of SSI effects generally results in period-lengthening and increased damping, which based on the format of code design spectra (e.g., National Building Code of Canada (NBCC) 1995) results in reduced spectral acceleration values. Although this may be true for various structures, it is an overly simplistic view, and has the effect of crippling design innovation, and blinding the analyst to important SSI response features (Mylonakis and Gazetas 2001; Allotey and El Naggar 2005b).

Performance-based design (PBD) requires designing structures to meet specified performance targets. The design method relies heavily on nonlinear analysis procedures and requires the analysis of the entire soil-structure system. The advent of this design philosophy has renewed the need to revisit simplified modeling approaches, with the aim of developing robust and efficient analysis tools for modeling SSI problems. In this regard, the nonlinear Winkler model has received the most attention and has been the focus of several recent studies (e.g., Boulanger et al. 1999; Gerolymos and Gazetas 2005; Allotey and El Naggar, 2005a). However, in most studies, it is used for modeling soil-pile-structure interaction (SPSI) problems and has not been widely used in modeling soil-foundation-structure interaction (SFSI) problems.

---

<sup>1</sup>Postdoctoral Fellow, Earthquake Engineering Research Facility, Dept. Civil Engineering, University of British Columbia, Vancouver, BC, V6T 1Z4, & Geotechnical Research Center, Dept. of Civil & Environmental Engineering, University of Western Ontario, London, Ontario, N6A 5B9

<sup>2</sup>Professor, Geotechnical Research Center, Dept. of Civil & Environmental Engineering, University of Western Ontario, London, Ontario, N6A 5B9

Under lateral cyclic motion, the response of spread footings is generally nonlinear involving horizontal displacement, settlement and rocking; part of the response is the possible dissipation of a considerable amount of energy. The nonlinear Winkler model can simulate progressive mobilization of plastic capacity, settlement and horizontal displacement and is therefore capable of modeling SFSI problems. In most SFSI studies, it has been used to simulate either the linear or nonlinear rocking response of structures, e.g., Psycharis and Jennings (1984), Chopra and Yim (1984), Filiatrault et al. (1992) and Anderson (2003). These studies have shown the suitability of the model to satisfactorily model the rocking response of the SFSI problems studied.

The overall objective of a larger study being undertaken by the authors is to promote the use of the nonlinear Winkler model for the analysis of the total SFSI problem, i.e., for the analysis of the horizontal, vertical and rotational response modes. This follows the guidelines given in the National Earthquake Hazard Reduction Program (NEHRP) FEMA 273 & 274 documents (BSSC 1997) that recommends the nonlinear Winkler foundation approach for the analysis of SFSI problems. Specifically, this paper presents relevant equations needed for estimating stiffness and bearing capacity distributions, and then points out some strengths and limitations of the modeling approach presented in the FEMA 273/274 documents. The paper makes use of the nonlinear Winkler model developed by Allotey and El Naggar (2005a) and integrated into the nonlinear structural analysis program, SeismoStruct (SeismoSoft 2003).

### Modeling Methods

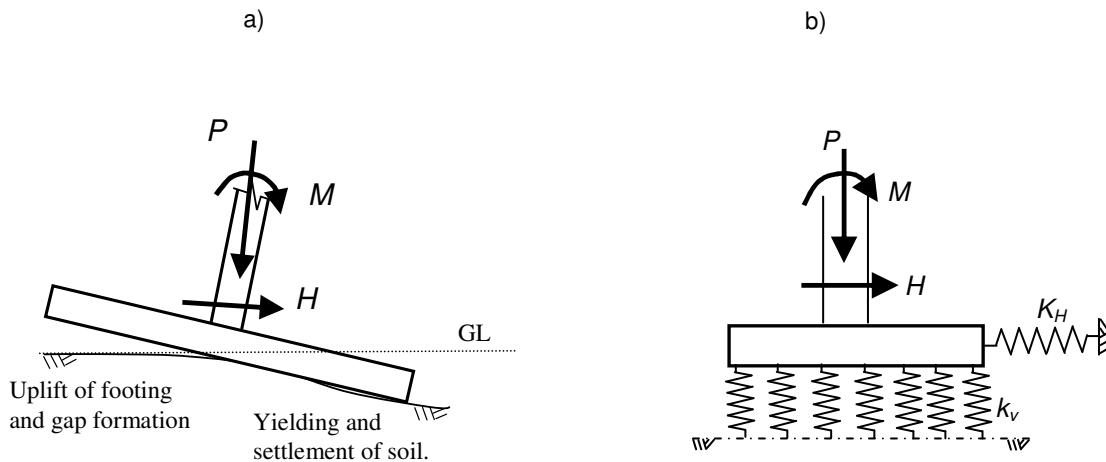


Figure 1. a) Schematic of foundation under horizontal, vertical and moment actions; b) schematic of recommended FEMA 273/274 Winkler modeling approach.

Fig. 1a shows the various vertical, horizontal and moment actions a footing is subjected to under lateral cyclic motion. As shown, the behaviour of the foundation can be very nonlinear due to factors such as foundation uplift, soil yielding and foundation settlement and permanent horizontal displacements and rotations. The FEMA 273/274 guidelines recommend that the foundation can be modeled as shown in Fig. 1b. The figure shows that the horizontal response is modeled with an independent horizontal spring that is uncoupled from the vertical and rotational responses.

The FEMA 273/274 design guidelines recommend using half-space solutions (e.g., Gazetas 1991) for the estimation of foundation stiffnesses, and standard bearing capacity superposition formulae (e.g., Vesic 1973) for the estimation of the BC under concentric loading. Foundation stiffnesses and BC can also be estimated from experiments such as: plate load tests, consolidation tests, triaxial tests, California bearing ratio (CBR) tests, etc.

The distribution of stiffness and BC under the foundation depends on the stress distribution under both working and ultimate conditions, respectively. The stress distribution underneath a foundation is, however, difficult to predict and depends on factors such as soil type and load level. Elastic solutions predict a theoretical convex parabolic stress distribution with infinite stresses at the edges, which in practice are limited to a finite value by local yielding (Shultze 1961). For ultimate loading conditions plastic solutions also predict a linear-to-concave parabolic distribution of stress (Kerr 1989). The distribution of stiffness and BC can therefore be quite variable and must be taken into account in SFSI analysis. It is therefore useful to have generalized equations that are capable of representing various shapes and can be easily used in a sensitivity analysis.

### Development of Distribution Functions for Rectangular Foundations

For a rigid rectangular foundation with plan dimensions  $2a$  and  $2b$  along the  $x$  and  $y$  axes, respectively, the vertical and rotational stiffnesses, and ultimate load can be given by:

$$K_v = \iint_A k_v(x, y) dx dy \quad (1a)$$

$$K_{\theta_x} = \iint_A k_v(x, y) y dx dy \quad (1b)$$

$$K_{\theta_y} = \iint_A k_v(x, y) x dx dy \quad (1c)$$

$$P_u = \iint_A q_u(x, y) dx dy \quad (2)$$

where  $k_v(x, y)$  and  $q_u(x, y)$  are functions representing the spatial distribution of the subgrade modulus,  $k_v$ , and the ultimate pressure,  $q_u$ . Candidate functions for  $k_v$  and  $q_u$  should be capable of modeling shapes ranging from concave to convex curved surfaces. Two possible functions are (Allotey 2006):

$$\zeta(x, y) = \zeta_o \left[ 1 + \frac{f_{1\zeta}}{(1+1/\vartheta_r)} \left( \left( \left| \frac{x}{a} \right| \right)^{n_\zeta} + \frac{1}{\vartheta_r} \left( \left| \frac{y}{b} \right| \right)^{n_\zeta} \right) \right] \quad (3a)$$

$$\zeta(x, y) = \zeta_o \left[ 1 + \frac{f_{1\zeta}}{(1+1/\vartheta_r)} \left( \left( 1 + \frac{1}{\vartheta_r} \right) - \left( \left( \left| \frac{x}{a} \right| \right)^{n_\zeta} + \frac{1}{\vartheta_r} \left( \left| \frac{y}{b} \right| \right)^{n_\zeta} \right) \right) \right] \quad (3b)$$

where  $\zeta$  represents  $k_v$  or  $q_u$ ,  $\vartheta_r = b/a$  is the aspect ratio,  $n_\zeta$  is a curve shape parameter, and  $f_{1\zeta}$  is a scale multiplier. Since  $\zeta_o > 0$ , Eq. 3a is convex-shaped and positive-definite for  $f_{1\zeta} > 0$ ; for  $f_{1\zeta} < 0$ , the function is concave-shaped but not positive-definite. Similarly, Eq. 3b is concave-shaped and positive-definite for  $f_{1\zeta} > 0$ , and convex-shaped but not positive-definite for  $f_{1\zeta} < 0$ . For  $f_{1\zeta} = 0$ , both functions are flat surfaces.

If the average and edge values of  $k_v$  and  $q_u$  are known, Eqs. 1a and 2 can be used in combination with either Eqs. 3a or 3b to derive expressions for  $k_v(\xi_r, \eta_r)$  and  $q_u(\xi_r, \eta_r)$ , where  $\xi_r = x/a$  and  $\eta_r = y/b$ , i.e.,

$$k_v(\xi_r, \eta_r) = \frac{(n_k + 1)k_{v-av}}{(1 + \vartheta_r)(f_{1k} + n_k + 1)} \left[ (1 + \vartheta_r) + f_{1k} \left( \vartheta_r (|\xi_r|)^{n_k} + (|\eta_r|)^{n_k} \right) \right] \quad (4a)$$

$$q_u(\xi_r, \eta_r) = \frac{q_{u-av}}{n_q} \left[ (1 + n_q) - f_{2q} + \frac{(1 + n_q)(f_{2q} - 1)}{(1 + \vartheta_r)} \left( \vartheta_r (|\xi_r|)^{n_q} + (|\eta_r|)^{n_q} \right) \right] \quad (4b)$$

where, Eqs. 4a and 4b are based on Eqs. 3a and 3b, respectively. In the equations,  $k_{v-av}$  and  $q_{u-av}$  are the average stiffness and bearing capacity,  $f_{1k}$  and  $f_{2q}$  are scale parameters with  $f_{1k} = f_{1\zeta} = (k_v(1, 1) - k_v(0, 0))/k_v(0, 0)$  and  $f_{2q} = (q_u(1, 1) - q_u(0, 0))/q_u(0, 0)$ , and  $n_k$  and  $n_q$  are curve shape parameters.  $q_u(\xi_r, \eta_r)$  is concave-shaped and positive-definite when  $0 \leq f_{2q} < 1$ .

With the definition of  $k_v(\xi_r, \eta_r)$ , the rotational stiffness can be derived using  $k_v(\xi_r, \eta_r)$  in conjunction with Eq. 1b or 1c. For example, with Eq. 4a and Eq. 1c,  $K_{\theta_y}$  can be derived as:

$$K_{\theta_y} = \frac{4a^3 b k_{v_{av}}}{3} \left[ \frac{1 + f_{1k} (3\vartheta_r (n_k + 1) + (n_k + 3)) / ((n_k + 3)(n_k + 1)(1 + \vartheta_r))}{1 + f_{1k} / (n_k + 1)} \right] \quad (5)$$

As  $f_{1k}$  and  $n_k$  become large, the limit of the expression in brackets gives  $(3\vartheta_r + 1) / (\vartheta_r + 1)$ . For large aspect ratios, this converges to 3, and  $K_{\theta_y} = K_v a^2$ . A similar expression could be also derived for  $K_{\theta_x}$ .

Fig. 2a compares the predicted limiting rotational stiffness with finite element/boundary element (FE/BE) results, and  $K_v$  and  $K_{\theta_y}$  calculated from the approximate formulae given by Pais and Kausel (1988), i.e.,

$$K_v = \frac{Ga}{(1 - \nu_s)} (3.1\vartheta_r^{0.75} + 1.6) \quad (6a)$$

$$K_{\theta_y} = \frac{Ga^3}{(1 - \nu_s)} (3.2\vartheta_r + 0.8) \quad (6b)$$

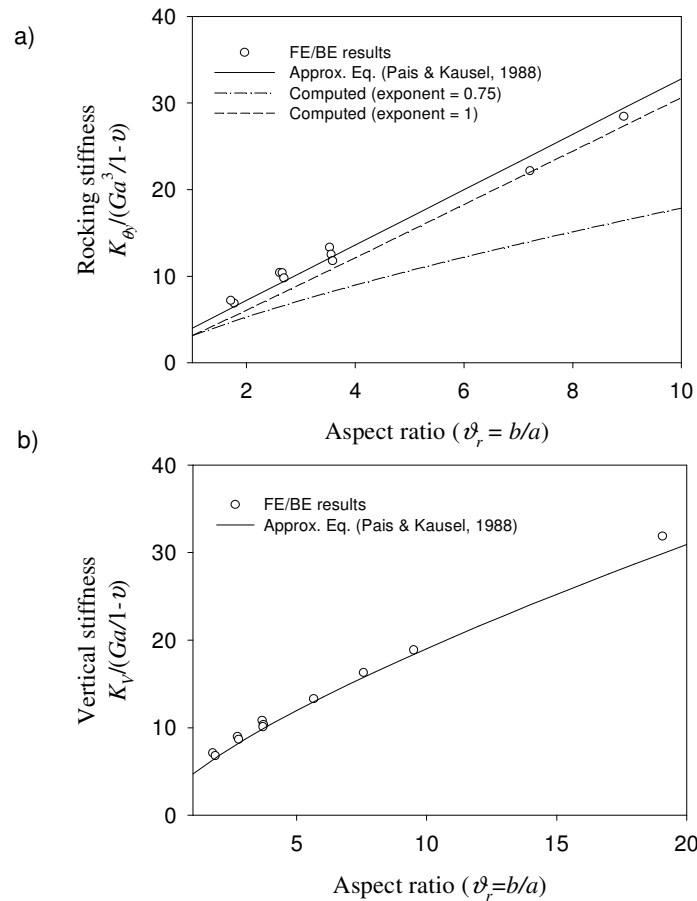


Figure 2. Variation of homogenous halfspace static stiffnesses for a rectangular foundation with aspect ratio: a) vertical stiffness; b) rocking stiffness.

It can be noted from the figure that the computed curve using Eq. 5 diverges from Pais and Kausel's solution as the aspect ratio increases. Varying the exponent in Pais and Kausel's expression for  $K_v$  from 0.75 to 1, the agreement between the computed curve and the results of Pais and Kausel improves, showing that the observed divergence is due to the difference in the exponents of Eqs. 6a and 6b.

Furthermore, from Fig. 2b, using an exponent of 1 in Eq. 6a does not significantly alter the agreement between  $K_V$  obtained from the FE results and Pais and Kausel's approximate solution. These comparisons therefore confirm the suitability of the chosen distribution functions.

### SSG02 Centrifuge Experiment

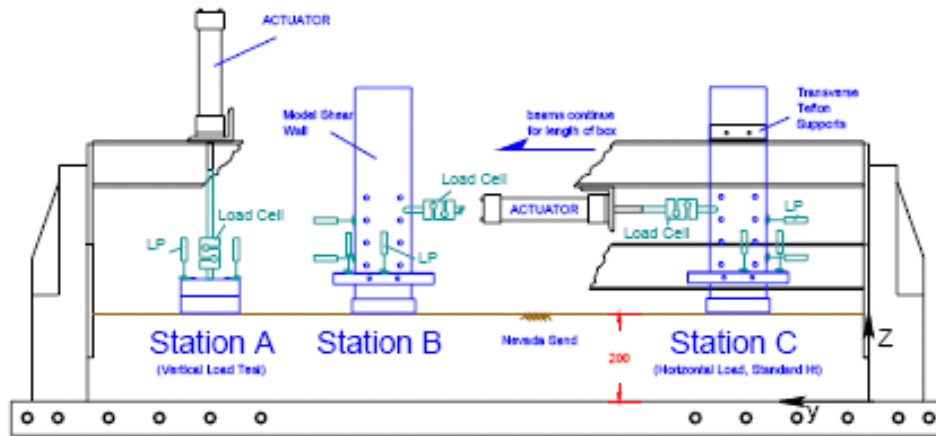


Figure 3. Side view of model container with selected wall-footing locations and typical instrument locations for SSG02 slow-cyclic tests (after Gajan et al. 2003).

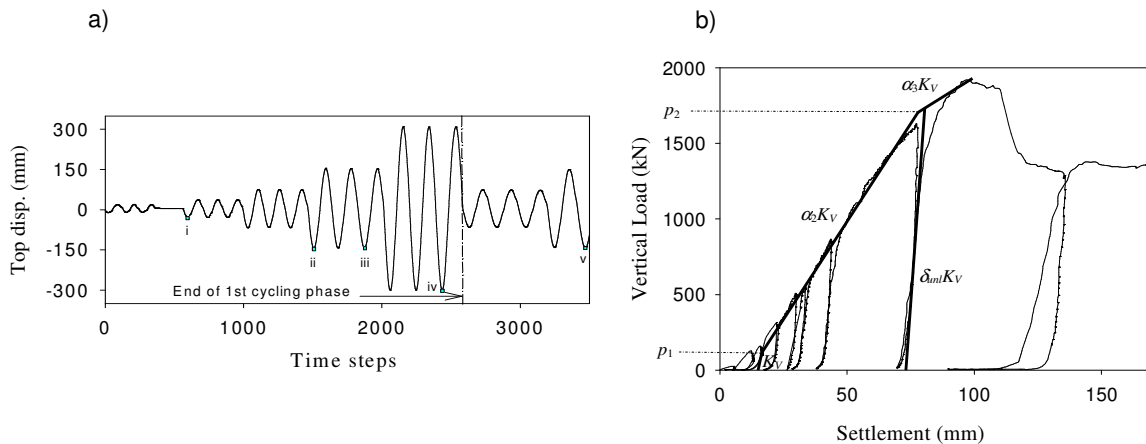


Figure 4. SSG02 Station B test: a) Input displacement time-history; b) vertical cyclic load-deformation response.

The SSG02 centrifuge experiment was conducted at the centrifuge facility of the University of California, Davis. It was part of a larger SFSI project involving the testing of several SFSI systems. The test considered in this study is a slow-cyclic horizontal test (frequency = 0.02 Hz) conducted at Station B on the test bed (Fig. 3). Apart from radiation damping effects, the tests are representative of the actual SFSI response that occurs under earthquake loading. The structure was a 10 m wall on a 2.67 m x 0.69 m spread footing (all prototype units) with a structural weight of 280 kN. The load was applied in the lengthwise direction of the wall at a distance of 4.9 m above the base. The input displacement history was a sinusoidal input displacement history with a maximum displacement of 310 mm (Fig. 4a). The entire loading history was repeated, however, only a section of the second part is shown in Fig. 4a. The underlying soil was a 200 mm thick bed of dry Nevada sand with an average relative density of 80%. The properties of the sand were:  $D_{50} = 0.15$  mm; coefficient of uniformity;  $C_u = 1.06$ ; specific gravity,  $G_s = 2.67$ ;  $e_{min} = 0.559$  and  $e_{max} = 0.871$  (Gajan et al. 2003). Also, the frictional angle back-calculated from vertical load tests using BC superposition formulae was  $42^\circ$ .

## Model Description and Parameter Estimation

The foundation was modeled in the lengthwise direction with stiffness and BC distribution functions integrated in the orthogonal direction. Fifty-one vertical springs were placed under the foundation with a single horizontal spring placed at the center node. The springs in the middle zone were spaced at two times the spacing of the springs in the edge zone. The multi-linear nonlinear Winkler model by Allotey and El Nagggar (2005a) was used to model the vertical springs, whereas, a Ramberg-Osgood (RO) hysteretic model was used to represent the horizontal spring.

The relevant input parameters used in the analysis are presented in Table 1. These were chosen as the best-estimate values based on the vertical load-deformation test (similar to plate load test) results presented in Fig. 4b. From the figure, the BC was found to be 1920 kN, implying a concentric vertical load factor of safety (FS) of 6.8. A uniform distribution of stiffness and BC was used; this was justified since based on an aspect ratio of 4.1 Eqs. 4a and 4b are almost uniform. In other words, the results for a convex parabolic distribution of stiffness (i.e.,  $n_k = 2$ ,  $f_{2k} = 4$ ) and a concave parabolic distribution of BC (i.e.,  $n_q = 2$ ,  $f_{2q} = 0$ ), are very similar to those obtained for the uniform distribution.

Table 1. Vertical and horizontal springs model parameters.

Vertical	
<u>Stiffness/BC distribution parameters</u>	
$k_{v,av}$ (MN/m <sup>3</sup> )	200
$q_{u,av}$ (kN/m <sup>2</sup> )	980
Stiff. dist.	uniform
BC dist.	uniform
<u>Curve parameters</u>	
$p_1$	0.05
$p_2$	0.8
$\alpha_2$	0.3
$\alpha_3$	0.03
$\delta_{unl}$	3
$\Lambda$	0.1
$\lambda_f$ ( $\lambda_s=1$ )	
(1)	0
(2)	$0.8 \frac{\sigma_r^4}{\zeta_r^4}$
Horizontal	
$K_H$ (MN/m)	80 <sup>+</sup>
$r_o$	15
$P_{yH}$ (kN)	70

Given as a ratio of the ultimate load

<sup>+</sup> Value represents the case  $K_H = 0.4K_V$

The loading curve parameters for the vertical springs were obtained from the unload-reload curve and the backbone curve of the vertical load test (Fig. 4b). The unload stiffness multiplier that relates the stiffness of the unload curve to the backbone curves,  $\delta_{unl}$ , was estimated to be 3. The cyclic curve shape parameter  $\Lambda$  was taken as 0.1 based on the recommended values given in Allotey (2006). Also, two cases were chosen for the cyclic curve shape parameters  $\lambda_s$  and  $\lambda_f$ : Case (1) referring to the traversal of the full gap distance developed due to foundation uplift; and Case (2) referring to the phenomenon of "soil squeeze out" due to asymmetric loading (Allotey 2006). The initial stiffness of the horizontal spring was estimated from half-space recommended stiffnesses given by Gazetas (1991), i.e.,  $K_H \approx 0.78K_V$ . A value of  $K_H = 0.4K_V$  was also used based on findings from other case studies (Allotey 2006).

## Results and Discussion

The results of the analysis are presented in Figs. 5 – 7. Fig. 5 shows the moment-rotation response including  $P$ - $\delta$  effects; a good agreement between the measured and computed results can be noted. The results presented are for case (2), which as noted from other case studies (Allotey 2006), gives a better prediction of the moment-rotation response. Also, the measured and computed responses show a strain-softening response at larger rotations, which can be attributed to the influence of  $P$ - $\delta$  on the response. It is therefore important that secondary order ( $P$ - $\delta$ ) effects be duly accounted for in all SFSI analysis.

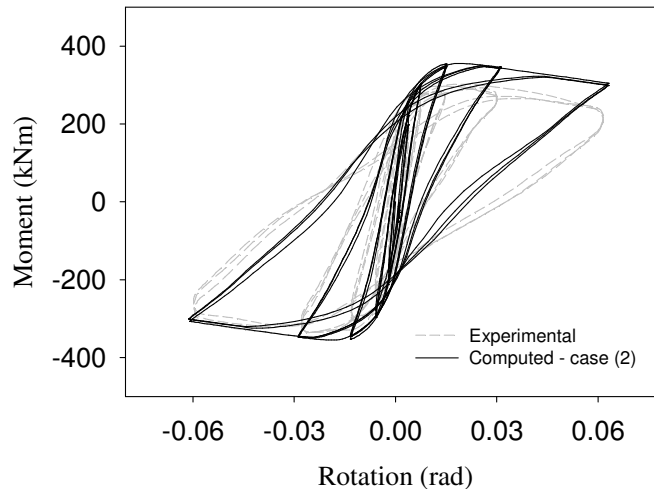


Figure 5. Comparison of experimental and computed moment-rotation results including  $P$ - $\delta$ .

Fig. 6 shows a comparison between the measured and predicted horizontal force-displacement responses. The results show that whereas cyclic horizontal displacements are well predicted, permanent horizontal displacements are not. This appears to be due to the lack of adequate coupling between the horizontal and vertical-rotational responses. This can only be improved by introducing a greater degree of coupling, and is a limitation of the modeling approach that should be noted. Similar to other case studies (Allotey 2006), initial stiffness estimates of  $K_H = 0.4K_V$  gave better predictions than elastic solution estimates.

The corresponding settlement-rotation response is also presented in Fig. 7. The general settlement pattern can be noted to be well-predicted, however, the final settlement is under-predicted by about 10 mm. Nonetheless, this prediction is better than those obtained by Gajan et al. (2005) with their macro-element model that accounts for coupling between the various responses. On the other hand, as a result of the higher degree of coupling inherent in their model, their model gave good predictions of the permanent horizontal displacement.

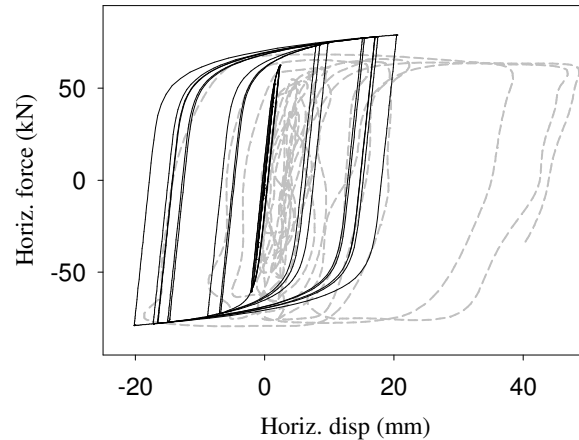


Figure 6. Comparison of experimental and computed horizontal force-displacement response.

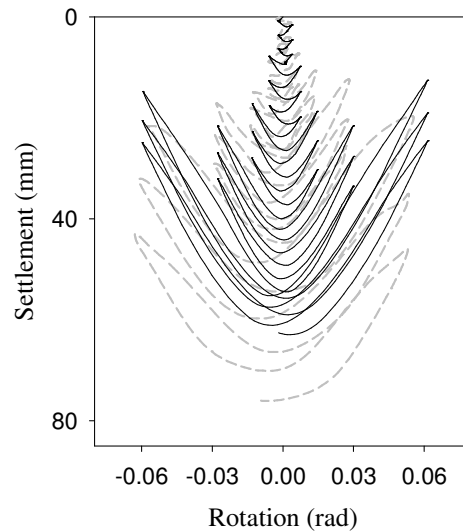


Figure 7. Comparison of experimental and computed settlement-rotation response.

### Conclusions

This paper discussed various issues relevant to the modeling of SFSI problems with the nonlinear Winkler modeling approach. Two generalized equations for rectangular foundations that can be used for either stiffness or BC distribution were initially presented. These equations allow for easier performance of sensitivity analysis studies on the effect BC and stiffness distribution variability have on the computed response. This is especially important, since in practice, both distributions are not known with certainty apriori.

The paper then focused on using the nonlinear Winkler modeling approach given in the FEMA 273/274 design guideline - with best-estimates of stiffness and BC - for the analysis of the SSG02 SFSI case study. The best-estimate parameters for the vertical springs were obtained from the vertical-load deformation response, and the horizontal was based on elastic solution estimates. The results obtained are summarized as follows.

- i. The modeling approach presented in the FEMA 273/274 guideline was able to give good predictions of the moment-rotation and settlement-rotation responses, even when secondary moment effects were significant.
- ii. Although, cyclic horizontal displacements were well-predicted, permanent horizontal

displacements were not. This is attributed to the limited coupling between the horizontal and vertical-rotational responses inherent in the modeling approach. This must therefore be noted when using the modeling approach in practice.

- iii. The observed actual initial horizontal uncoupled spring stiffness,  $K_H$ , was noted to be less than elastic solution estimates that are recommended in the FEMA 273/274 design guideline. This could be attributed to the fact that the elastic solution estimates are obtained for a full-contact horizontal-only response mode. This is in contrast with the partial-contact coupled SFSI response that really occurs.

### Acknowledgements

The authors would like express their deep appreciation to Drs. Stelios Antoniou and Rui Pinho of SeismoSoft for offering valuable help with the modeling of the SSG02 case study. Also, the authors would like to thank Prof. Bruce Kutter and Dr. Siva Gajan of the Center for Geotechnical Modeling, University of California, Davis, for providing the SSG02 test data.

### References

- Allotey, N. K., 2006. Nonlinear soil-structure interaction in performance-based design. *Ph.D. Thesis*, University of Western Ontario, London, Ontario.
- Allotey, N. K. and El Naggar, M. H., 2005a. Cyclic soil-structure interaction model for performance-based design. *Proceedings of Geotechnical Earthquake Engineering Satellite Conference, TC4*, ISSMGE, Osaka, Japan, 30-37.
- Allotey N. K and El Naggar M. H., 2005b. Soil-structure interaction in performance-based design - a review. *Predictions, Analysis and Design in Geomechanical Applications, Proceedings of 11th International Conference on Computational Methods and Advances in Geomechanics*, Torino, Italy, 3, 595-602.
- Anderson, D. L., 2003. Effect of foundation rocking on the seismic response of shear walls. *Canadian Journal of Civil Engineering*, 30, 360-365.
- Boulanger, R. W., Curras, J. C., Kutter, B. L., Wilson, D. W. and Abghari, A., 1999. Seismic soil-pile-structure interaction experiments and analysis. *Journal of Geotechnical and Geoenvironmental Engineering*, ASCE, 125(9), 750-759.
- Building Seismic Safety Council (BSSC), 1997. *FEMA 273/274 - NERHP Guidelines for the Seismic Rehabilitation of Buildings*, Vol. I – Guidelines, Vol. II – Commentary, Washington DC.
- Chopra, A. K. and Yim, C. S., 1984. Earthquake responses of structures with partial uplift on Winkler foundation. *Earthquake Engineering and Structural Dynamics*, 12, 265-281.
- Filiatrault, A., Anderson, D. L. and DeVall, R. H., 1992. Effect of weak foundation on the seismic response of core-wall type buildings. *Canadian Journal of Civil Engineering*, 19, 530-539.
- Gajan. S., Phalen. J. D. and Kutter. B. L., 2003. Soil-foundation-structure interaction: shallow foundations. centrifuge data report for SSG02, *Report No. UCD/CGMDR-03/01*, Center for Geotechnical Modeling, University of California, Davis.
- Gajan. S., Thomas. J. M. and Kutter. B. L., 2005. Physical and analytical modeling of cyclic load-deformation behaviour of shallow foundations. *Proceedings of 57th Annual Meeting of Earthquake Engineering Research Institute*, Mexico.

- Gazetas, G., 1991. Foundation vibrations, *Foundation Engineering Handbook*, Ch. 15, Ed. H. Y. Fang, van Nostrand Reinhold, New York.
- Gerolymos, N. and Gazetas, G., 2005. Phenomenological model applied to inelastic response of soil-pile interaction systems. *Soils and Foundations*, 45(4), 119-132.
- Kerr, A. D., 1989. Tests and analysis of footings on a sand base. *Soils and Foundations*, 29(3), 83-94.
- Pais, A. and Kausel, E., 1988. Approximate formulas for dynamic stiffnesses of rigid foundations. *Soil Dynamics and Earthquake Engineering*, 7(4), 213-228.
- Psycharis, I. N. and Jennings, P. C., 1984. Rocking of slender rigid bodies allowed to uplift. *Earthquake Engineering and Structural Dynamics*, 11, 57-76.
- Mylonakis, G. and Gazetas, G., 2000. Seismic soil-structure interaction: beneficial or detrimental? *Journal of Earthquake Engineering*, 4(3), 277-301.
- National Building Code of Canada (NBCC), 1995. NBCC Code and Commentary, *National Research Council of Canada, NRCC 38726: I-571*, Ottawa, Ontario.
- Schultze, E., 1961. Distribution of stress distribution beneath a rigid foundation. *Proceedings of 5th International Conference on Soil Mechanics and Foundation Engineering*, 6, 807-813.
- SeismoSoft, 2003. *SeismoStruct — A Computer Program for Static and Dynamic Nonlinear Analysis of Framed Structures*, Available online: <http://www.seismosoft.com>.
- Vesic, A. S., 1973. Analysis of ultimate loads on shallow foundations. *Journal of Soil Mechanics and Foundations Division, ASCE*, 98(SM3), 45-73.